



RESEARCH ARTICLE



WILEY

Influence of ocular dominance columns and patchy callosal connections on binocularity in lateral striate cortex: Long Evans versus albino rats

Adrian K. Andelin¹ | Zane Doyle¹ | Robyn J. Laing² | Josef Turecek³ | Baihan Lin⁴ | Jaime F. Olavarria¹

¹Department of Psychology and Behavior and Neuroscience Program, University of Washington, Seattle, Washington

²Department of Biological Structure, University of Washington, Seattle, Washington

³Department of Neurobiology, Harvard Medical School, Boston, Massachusetts

⁴Center for Theoretical Neuroscience, Zuckerman Mind Brain Behavior Institute, Columbia University, New York, New York

Correspondence

Jaime F. Olavarria, Department of Psychology, University of Washington, Seattle, WA, 98195-1525.

Email: jaime@uw.edu

Funding information

National Institute of Health Vision Training Grant, Grant/Award Number: T32 EY7031; National Institutes of Health, Grant/Award Number: R01NS070022; Royalty Research Fund award, University of Washington

Peer Review

The peer review history for this article is available at <https://publons.com/publon/10.1002/cne.24786>.

Abstract

In albino rats, it has been reported that lateral striate cortex (V1) is highly binocular, and that input from the ipsilateral eye to this region comes through the callosum. In contrast, in Long Evans rats, this region is nearly exclusively dominated by the contralateral eye even though it is richly innervated by the callosum (Laing, Turecek, Takahata, & Olavarria, 2015). We hypothesized that the inability of callosal connections to relay ipsilateral eye input to lateral V1 in Long Evans rats is a consequence of the existence of ocular dominance columns (ODCs), and of callosal patches in register with ipsilateral ODCs in the binocular region of V1 (Laing et al., 2015). We therefore predicted that in albino rats input from both eyes intermix in the binocular region, without segregating into ODCs, and that callosal connections are not patchy. Confirming our predictions, we found that inputs from both eyes, studied with the transneuronal tracer WGA-HRP, are intermixed in the binocular zone of albinos, without segregating into ODCs. Similarly, we found that callosal connections in albino rats are not patchy but instead are distributed homogeneously throughout the callosal region in V1. We propose that these changes allow the transcallosal passage of ipsilateral eye input to lateral striate cortex, increasing its binocularity. Thus, the binocular region in V1 of albino rats includes lateral striate cortex, being therefore about 25% larger in area than the binocular region in Long Evans rats. Our findings provide insight on the role of callosal connections in generating binocular cells.

KEYWORDS

columnar organization, eye-specific domains, interhemispheric connections, primary visual cortex, RRID:RGD_68073, Sprague-Dowley rat (RRID:RGD_70508), V1

1 | INTRODUCTION

In pigmented, hooded Long Evans rats, inputs from both eyes are anatomically and functionally segregated into ocular dominance columns (ODCs) in the central segment (CS) of striate cortex (V1) (Laing, Turecek, Takahata, & Olavarria, 2015). Interposed between the CS and the lateral border of V1, these authors identified a narrow strip of cortex, named lateral segment (LS), that is strongly, if not exclusively,

dominated by the contralateral eye. Moreover, callosal connections in V1 accumulate forming distinct patches that colocalize with ipsilateral ODCs in the CS, and a dense, continuous band that overlaps the region of contralateral eye input in the LS. This organization mirrors the close spatial relationship between eye-specific ODCs and callosal connections described previously in the cat (Olavarria, 2001, 2002), namely, callosal connections correlate with ipsilateral ODCs in regions

corresponding to the CS, and with contralateral ODCs in regions corresponding to the LS.

The observation that the LS in Long Evans rats is strongly dominated by the contralateral eye despite being richly innervated by the corpus callosum implies that callosal projections are unable to relay indirect input from the ipsilateral eye to the LS in the Long Evans strain of rats. Analysis of the relevant retinofugal and callosal circuits in Long Evans rats (Laing et al., 2015) led us to hypothesize that the presence of ODCs and patchy callosal connections *prevents* the transcallosal passage of ipsilateral eye input to lateral V1 in Long Evans rats, or equivalently, that lack of ODCs and patchy callosal connections *facilitates* the transcallosal passage of ipsilateral eye input to lateral V1. Rather than inducing the absence of ODCs in Long Evans rats, which would have required manipulations with unknown collateral effects, we chose to study albino rats because previous studies in these rats have reported that a region corresponding to the LS in lateral striate cortex is highly binocular, and that input from the ipsilateral eye to this region comes through the callosum (Diao, Wang, & Pu, 1983). We therefore predicted that albino rats lack ODCs, that is, input from both eyes intermix in the V1 binocular region, without segregating into ODCs, and that callosal connections in V1 are not patchy in this rat strain.

In agreement with Diao et al. (1983), our analysis of microelectrode recordings showed that evoked responses are predominantly binocular in lateral striate cortex of albino rats, and that transection of the callosum virtually eliminates input from the ipsilateral eye to this region. To test our anatomical predictions, we analyzed the patterns of retinal input to V1 in tangential cortical sections following monocular injections of the transneuronally transported tracer WGA-HRP. We also analyzed the patterns of callosal connections revealed following multiple intracortical injections of horseradish peroxidase (HRP). Confirming our predictions, we found that, unlike Long Evans rats, inputs from both eyes do not segregate into ODCs, but instead overlap throughout the CS of albino rats. Moreover, also unlike Long Evans rats, we found that callosal connections do not form distinct patches but are instead distributed throughout the CS of albino rats, overlapping the diffuse distribution of direct ipsilateral eye input in the CS. As a consequence of these changes, the binocular region in albino rats not only includes the CS but also the LS, being therefore larger in area size than the binocular region in Long Evans rats, which is largely restricted to the CS. These findings suggest that the capacity of callosal connections to contribute to the generation of binocular cells in rat striate cortex depends to a large extent on factors and constraints determining the modular architecture of eye-specific domains in striate cortex and the spatial correlation between these domains and the distribution of callosal connections.

2 | MATERIALS AND METHODS

This study used adult Long Evans pigmented (RRID:RGD_68073) and Sprague–Dawley albino (RRID:RGD_70508) rats (*Rattus*

norvegicus). Animal procedures were performed according to protocols approved by the Institutional Animal Care and Use Committee at the University of Washington and are in accordance with the animal care guidelines of the National Institutes of Health.

2.1 | Intraocular and intracortical injections of anatomical tracers and histochemical processing

Intraocular and intracortical tracer injections were performed under anesthesia induced and maintained with isoflurane (5 and 2.5%, respectively) in air. In 7 albino rats, a total volume of 6 μL of 3% HRP conjugated to wheat-germ agglutinin (WGA-HRP) in saline was pressure injected into one eye over 15 min through glass micropipettes (50–100 μm tip diameter). The injection site was ~ 2 mm posterior to the corneal limbus, at a depth of ~ 2 mm. Data on ipsilateral eye projections to V1 in 9 Long Evans rats obtained similarly by Laing et al. (2015) were analyzed for comparison. Due to its transneuronal transport property, WGA-HRP has been widely used in studies of retinohalamo-cortical projections and patterns of ODCs in a variety of species (see Laing et al., 2015, for references).

Callosal connections were labeled following multiple intracortical injections of HRP (Sigma Co, 25% in saline; total volume = 4.0 μL) into occipital cortex of Long Evans ($n = 8$) and albino ($n = 8$) rats. Injections were evenly spaced (0.2 μL each), at a depth of ~ 800 – $1,000$ μm . Previous studies at both light and electron microscopic levels have demonstrated that HRP is transported both anterogradely and retrogradely (Trojanowski, Gonatas, & Gonatas, 1981). HRP was pressure injected through glass micropipettes (50–100 μm tip diameter) over an area extending from ~ 2.0 to 7.0 mm lateral to the midline suture, and 0.0–6.0 mm anterior to lambda suture. The dura was kept intact and moist with saline. Following the injections, the bone chip was repositioned, and the skin was sutured by planes. Data on callosal connections in Long Evans rats obtained similarly by Laing et al. (2015) were analyzed for comparison.

Four days following intraocular injections of WGA-HRP and 2–3 days following intracortical injections of HRP, animals were deeply anesthetized with pentobarbital sodium (100 mg/kg i.p.) and perfused through the heart with 0.9% saline followed by 4% paraformaldehyde (PFA) in 0.1 M phosphate buffer (PB, pH 7.4). Cortices were separated from the brains and flattened for sectioning in the tangential plane, while the remainder of the brain was left intact for coronal sectioning. The flattened cortices were left between glass slides for 24 hr in 0.1 M PB, after which time the tissue was transferred to a 4% PFA in 0.1 M PB, 20% sucrose solution for 1 additional hour. Tissue blocks to be sectioned in the coronal plane were kept in 4% PFA in 0.1 M PB and 20% sucrose for one or more days. All tissue was cut using a freezing microtome at 60 μm thickness, and the sections were collected in 0.1 M PB. Sections were reacted for HRP with 3,3',5'-tetramethylbenzidine as the chromogen (Mesulam, 1978).

2.2 | Electrophysiology

Electrophysiological recordings in Long Evans and albino rats were performed under urethane anesthesia (1,200 mg/kg i.p.). Atropine sulfate (0.1 mg/kg i.p.) was used to reduce tracheal secretions. Body temperature was kept at 37 °C with a heating pad. Pupils were dilated with atropine sulfate ophthalmic solution (1%, Bausch and Lomb), and artificial tears (polyethylene glycol eye drops) and silicone oil was used to protect the corneas and the cerebral cortex, respectively. Prior to recording, the occipital cortex was exposed by drilling a window into the skull that extended from 2.0 to 7.0 mm in the mediolateral direction, and from the lambda suture to 5.0 mm in the anteroposterior direction. The dura mater was left intact. Multiunit activity was recorded with glass-insulated tungsten electrodes (1–2 M Ω ; FHC) positioned perpendicularly to the cortical surface, at depths of 500–600 μ m, and displayed on an oscilloscope and an audio monitor. Signals were filtered and amplified using a digital electrophysiology amplifier board (RHD 2132, Intan technologies, LLC) and USB interface board (RHD 2000 series, Intan Technologies, LLC), and stored on a computer for later analysis.

Full field visual stimuli were presented through custom-made eye covers housing a white LED for each eye. The eye covers ensured that each eye was stimulated independently from the other eye. A custom-made remote control simultaneously sent a signal to one LED as well as the electrophysiology interface board, allowing visually evoked responses to be time-locked to stimulation. Each eye was stimulated separately while the non-stimulated eye was occluded by covering it. Visual responses elicited from an eye ceased when the eye was covered, indicating that covering of the eyes was effective in preventing visual stimulation. Electrode penetrations, spaced at least 200 μ m apart, were arranged in a grid over the lateral half of V1.

The ocular preference of evoked response at recording sites judged to be within the CS and LS was assessed quantitatively in Long Evans ($n = 10$) and albino ($n = 5$) rats. In an additional group of albino rats ($n = 7$), we tested the effect of transecting the callosum on binocularity in V1. The splenium of the corpus callosum was transected at the beginning of the recording session by making a parasagittal cut with a #11 scalpel blade in the hemisphere opposite to the recordings, 1 mm lateral to the midline, 3 mm deep, and extending posteriorly from 3 to 6 mm measured from the bregma suture. Action potentials (APs) were collected after filtering and thresholding recording traces of neural activity using a custom Matlab script (ver 2015a; Mathworks). The spontaneous activity recorded during 300 milliseconds prior to stimulation was subtracted from responses recorded from each eye during the 300 milliseconds following stimulation onset. These time windows were chosen based on analysis of peak response times to visual stimulation. For each recording site, counts of the APs for each trial were summed and averaged for each eye. Using these values, a contralateral bias index (CBI) was calculated to evaluate the ocular preference of responses

within each of the cortical regions analyzed, according to the formula:

$$\text{CBI} = (\text{Rcontra} - \text{Ripsi}) / (\text{Rcontra} + \text{Ripsi}).$$

R denotes responses, measured as number of APs, for stimulations of either the contralateral or ipsilateral eye. This index ranges from -1 (purely ipsilateral response) to $+1$ (purely contralateral response). Values ~ 0 indicate balanced binocular responses.

Rats with and without callosal transection were perfused immediately at the end of recording sessions, and the recorded hemispheres were flattened for tangential sectioning. The callosotomy was inspected in coronal sections, and all cases analyzed ($n = 7$) had a complete transection of the splenium.

2.3 | Data acquisition and analysis

Prior to histochemical processing, the tangential sections from flattened hemispheres were digitally scanned at 2400 dpi for identification of the V1 border, which was revealed by the abrupt transition in the density of myelination pattern upon passing from striate cortex to extrastriate cortex (Figure 1e) (Laing et al., 2015; Laing, Bock, Lasiene, & Olavarria, 2012; Richter & Warner, 1974). The myelin pattern, optimally displayed in tangential sections passing through layer 4 (~ 500 – 650 μ m deep), was confirmed in two or more sections from the same animal. The V1 border (black line in Figure 1e) was delineated in the myelin pattern with the aid of the filter “trace contour” in Adobe Photoshop CS5 (Adobe Systems, CA). Further information for identifying the border of V1 was provided by the relationship that is known to exist between this border and distinct features of the callosal pattern in V1 (Laing et al., 2012; Olavarria & van Sluyters, 1985). Following the histological processing for anatomical tracers, digital images of the labeling patterns were obtained by scanning the sections (Epson 4990). The patterns of retino-geniculo-cortical projections labeled with WGA-HRP, and the patterns of HRP-labeled callosal connections were displayed either from one tangential section or from reconstructions of two superimposed sections. The digitized images of myelin and anatomical labeling patterns were aligned with each other in Adobe Photoshop, using the border of V1, the edges of sections, and radial blood vessels as fiducial markers. Since sections scanned to reveal the myelin pattern were subsequently reacted for HRP, aligned myelin and labeling images often came from the same sections. In all images, noise and Gaussian filters were applied to reduce sharp increases in density produced by blood vessels and other artifacts; high pass filters were applied to remove gradual changes in labeling intensity; and levels and brightness/contrast filters were used to enhance the images. All filters were applied to the entire images. ImageJ (ver 1.50e) was used to obtain 3-D surface plots of the patterns of ipsilateral eye input and callosal patterns in V1 and to analyze patchiness data. High-magnification images were obtained using a DMR Leica microscope coupled to a Leica DC 300F digital camera.

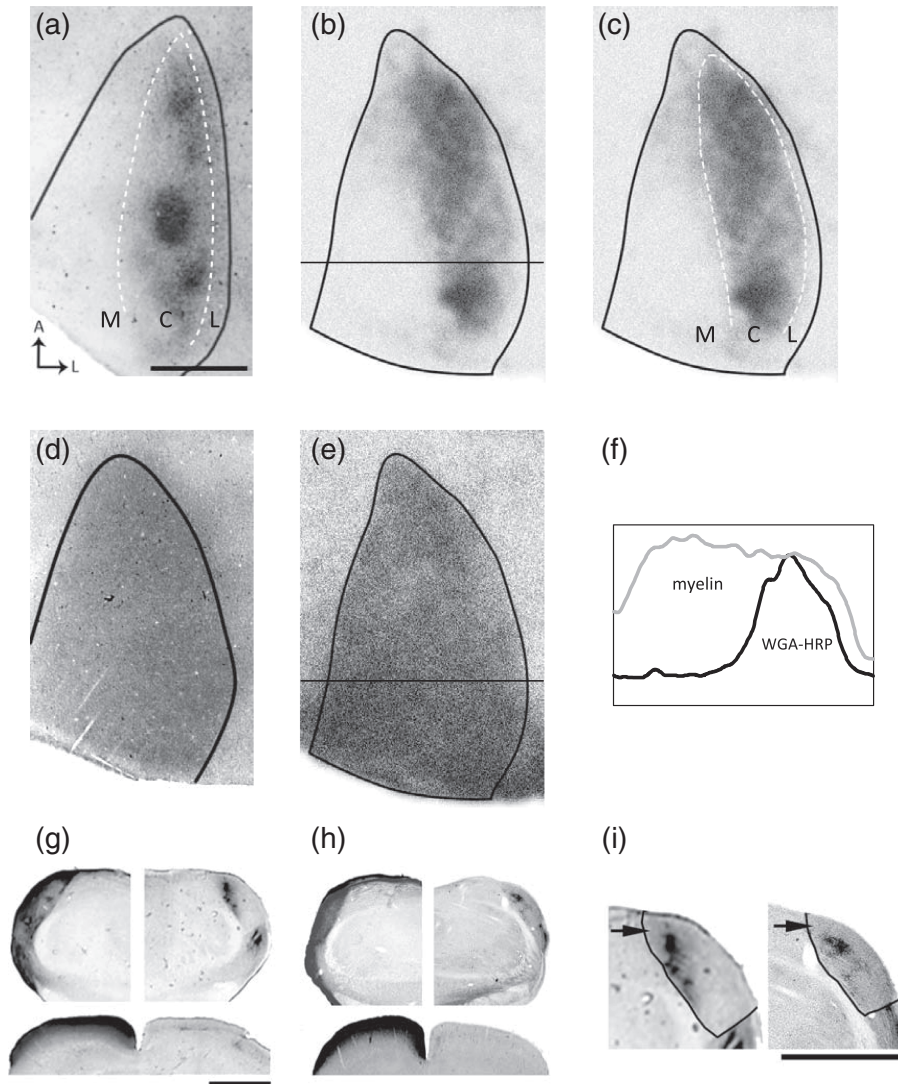


FIGURE 1 WGA-HRP labeling of retino-dLGN-V1 projections in Long Evans and albino rats. (a) Representative case of Long Evans ipsilateral eye labeling (adapted from Laing et al., 2015). Note the distinct labeled patches in the central segment of V1 (outlined by white segmented line). (b) Representative case of ipsilateral eye WGA-HRP labeling in V1 of albino rat. Note that the labeling is more widespread than in Long Evans rats. The black line indicates the border of V1 determined based on the myelin pattern from the same case as shown in (e) (see Materials and Methods). (c) the same case as in (b); the white segmented line delineates the WGA-labeled region in the central segment (see Materials and Methods). (d) Labeling in V1 contralateral to the eye injected with WGA-HRP for the albino case as shown in (b). (e) Myelin pattern of V1 for albino case as shown in (b). The border of V1 based on the myelin pattern is indicated by a black line (see Materials and Methods). (f) Plots of normalized mediolateral density profiles at the levels indicated in (b) and (e) show that the density of WGA-HRP labeling (black trace) declines more medially than that for the myelin pattern (gray trace), leaving a gap, about 0.20 mm in width, in lateral V1 of albino rats. (g) Labeling pattern in dLGN (top) and superior colliculus (SC, bottom) of Long Evans rat in (a). (h) Labeling pattern in dLGN and SC for albino case in (b). (i) Higher magnification of the dLGNs from the Long Evans and albino rats as shown in (g), (h), respectively. Arrows indicate dorsomedial region that remains unlabeled after intraocular injections of WGA-HRP into the ipsilateral eye in both rat strains. This dLGN region innervates lateral V1 (see refs. in text). Scale bars in (a), (g), and (i) = 1.0 mm. In (a) and (c), C, central segment; L, lateral segment; M, medial segment

2.4 | Analysis of patchiness in the patterns of ipsilateral retino-geniculo-cortical projections and callosal connections

2.4.1 | Area method

The degree of patchiness of ipsilateral eye and callosal labeling patterns in V1 was quantitatively evaluated using a patchiness index area (PIA) calculated using the formula: $PIA = 1 - SM/SI$

SI is the surface area of the 3D density profile of the labeling distribution over the target region, while SM is the surface area of the projection of SI onto a 2-D plane. Values of PIA approaching zero indicate low patchiness, that is, the labeling density landscape fluctuates little (the area of SI approaches that of SM), while increasing values of PIA indicate larger fluctuations in the labeling density landscape (i.e., area of SI is larger than that of SM). SI and SM were calculated using a custom Matlab script. To account for differences in gray scale

values across cases, the gray scale values in each image were normalized by dividing them by the mean gray scale value in the image.

2.4.2 | SD method

The degree of patchiness in labeling distributions was also evaluated by calculating the SDs of the gray value distributions: Images with large variations in labeling density (i.e., high patchiness) contain a wide range of gray values and have large SD, whereas images with uniform distributions (i.e., low patchiness) are more restricted in their range of gray values and have smaller SD. To examine whether increases in the tracer reaction times affect the grayscale values, we compared the mean grayscale values across the entire tissue sample across groups and found that the variance both within and between groups was not statistically significant ($p > .05$)

In the electrophysiology experiments, the locations of recording sites along with local blood vessels used as reference were marked on digital images of the intact cortical surface taken immediately before recordings began. The images were correlated with images of the most superficial tangential sections, and the recording sites were matched to the patterns made by electrode penetrations in these sections. The first tangential sections were aligned with deeper sections using the pattern of penetrating blood vessels, section borders, and other landmarks. Following histological processing, the binocularity at recording sites judged to be in the CS and LS was calculated. The border of V1 was determined using the myelin pattern (Figure 4a), while the borders of CS and LS were estimated based on measurements from cases used to demonstrate the patterns of cortical WGA-HRP labeling (e.g., Figure 1c). Intraocular injections of WGA-HRP were not used to identify the borders of CS and LS in the recording experiments in order to avoid the risk of retinal damage, which could have interfered with the recording of evoked responses from the injected eye. In intact albinos, 10 sites in the LS and 19 sites in the CS were analyzed. In albinos that underwent callosotomy, 11 sites in the LS and 25 sites in the CS were analyzed. In Long-Evans rats, a total of 5 sites fell within the LS, and 33 sites fell within the CS. Only penetrations judged to be oriented perpendicularly to the cortical surface were analyzed.

3 | RESULTS

3.1 | Tripartite subdivision of V1

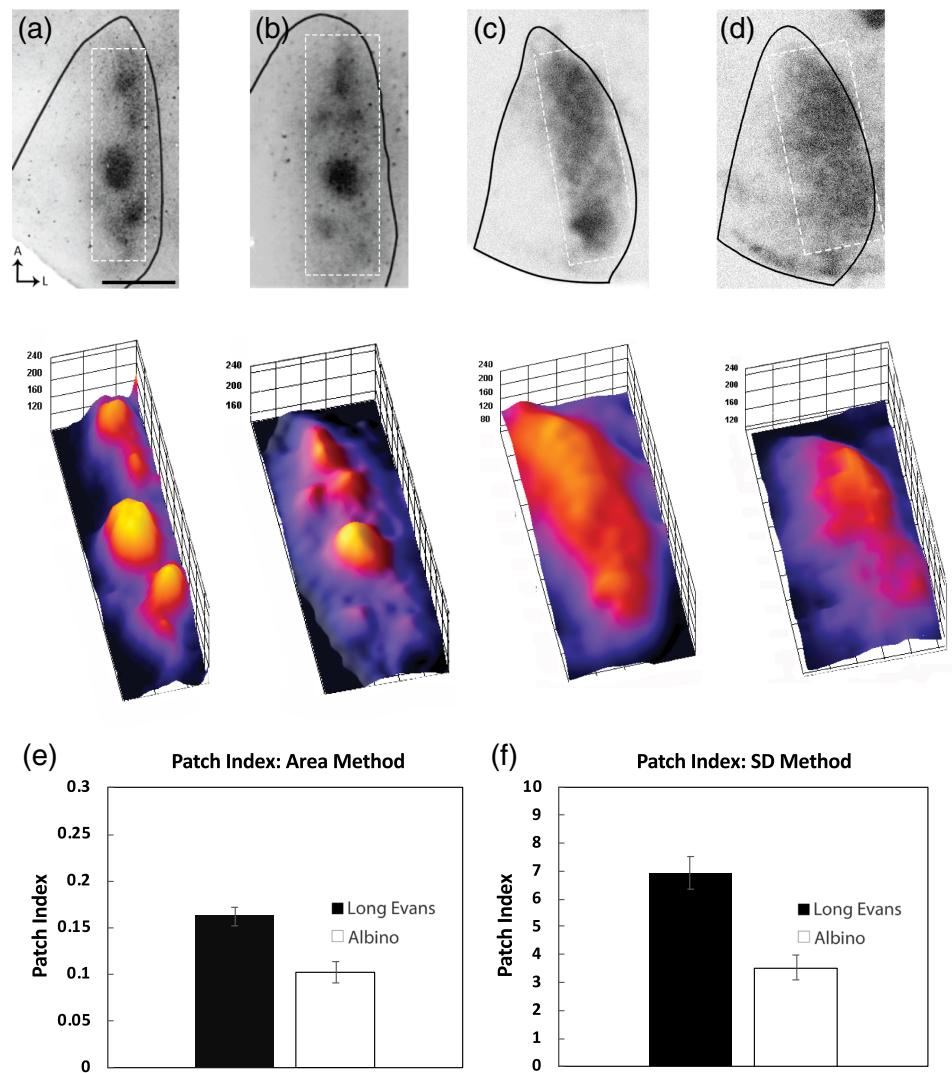
To investigate the distribution of retino-geniculo-cortical input to striate cortex in albino rats, we injected the anatomical tracer WGA-HRP into one eye and analyzed the pattern of WGA labeling in tangential cortical sections. The transneuronal transport property of WGA-HRP has been demonstrated at both the optical and structural level (Itaya & van Hoesen, 1982), and, as in Long Evans rats, the pattern of anterogradely labeled geniculo-cortical axon terminals in V1 was most distinct at the level of layer 4 (~500–650 μm) (Itaya & van Hoesen, 1982; Kageyama, Gallivan, Gallardo, & Robertson, 1990; Laing et al., 2015). In the hemisphere ipsilateral to the injected eye (Figure 1b),

the transneuronally transported tracer accumulated in a restricted portion of V1, about 1 mm wide, which was separated from the lateral border of V1 by a narrow strip of cortex, about 0.20 mm at its widest level, where the tracer density was markedly reduced or at background levels. Figure 1c shows the contour of the WGA-HRP labeled area (dashed white line), which was traced by eye and confirmed using the filter “trace contour” in Adobe Photoshop. The border of V1 in Figure 1b,c corresponds to the border determined from the myelin pattern (black line in Figure 1e). Figure 1f compares the normalized density profiles across both the ipsilateral WGA-HRP labeling pattern (Figure 1b) and the myelin pattern from the same hemisphere (Figure 1e) at the levels indicated. Figure 1f illustrates that the density of WGA-HRP labeling decreases before reaching the lateral border of V1 as indicated in the myelin pattern, leaving a gap, approximately 0.20 mm in width, of reduced labeling corresponding to the LS. The labeling density was also absent or markedly reduced in the remaining, medial portion of V1, which extended to the medial border of V1 (Figure 1b). Thus, on the basis of the transneuronal transport of WGA-HRP from the ipsilateral eye, in albino rats, as in Long Evans rats (Figure 1a), V1 can be divided into three main subdivisions or segments: (a) The CS, defined as the area receiving the bulk of ipsilateral retino-thalamo-cortical projections (outlined by white segmented lines in Figure 1a,c); (b) The Medial Segment (MS), located medial to the CS, presumably representing the peripheral monocular visual field; and (c) The LS, located between the CS and the lateral border of V1. On average, the area of the LS is approximately 25% of the area of the CS. The WGA-HRP labeling patterns illustrated in Figure 1a,b,d come from sections cut at the level of layer 4.

3.2 | Eye-specific projections

In Long Evans rats (Figure 2a,b), the ipsilateral eye projection forms distinct patches in V1, which, as a group, occupy only about one-third of the total surface area of the CS (Laing et al., 2015), while in albino rats, distinct labeled patches are not observed in the CS. Instead, the WGA-HRP labeling is distributed rather uniformly, occupying the entire CS (Figures 1c, 2c,d). In the hemisphere contralateral to the injected eye in albino rats, the WGA-HRP labeling in sections taken at the level of layer 4 is distributed uniformly throughout V1, including the LS (Figure 1d). In particular, restricted regions of reduced labeling (corresponding to territory innervated by the non-injected eye) are not observed in the CS of albino rats, as reported in Long Evans rats (Laing et al., 2015). Comparing the labeling patterns in the hemispheres ipsilateral and contralateral to the eye injected with WGA-HRP indicates that the LS receives little or no direct (i.e., retino-geniculo-cortical) input from the ipsilateral eye, consistent with the report by Diao et al. (1983) that in albino rats, ipsilateral input to lateral V1 comes via the corpus callosum. Moreover, this comparison indicates that direct contralateral and ipsilateral eye projections overlap in the CS, suggesting that these inputs intermix in this region, rather than segregate into separate domains as in Long Evans rats (Laing et al., 2015).

FIGURE 2 WGA-HRP labeling patterns and 3D surface plots for Long Evans and albino rats. (a) and (b) two cases of Long Evans rats (top, adapted from Laing et al., 2015) and respective 3D surface plot reconstructions of the labeling pattern (bottom). (c), (d) two cases of albino rats (top) and respective 3D surface plot reconstructions of labeling patterns. The 3D plots derive from the areas delineated with dashed lines in the top row. Scale bar = 1.0 mm. (e), (f) patch index: Area method and SD method for ODCs. (e) Average values of patch index area method. Long Evans rats ($n = 9$) are significantly different from albino group ($n = 7$) ($p = .002$). (f) Average patch index SD method. Long Evans rats ($n = 9$) are significantly different from the albino group ($n = 7$) ($p = .001$). Error bars in both graphs denote SEM for each group



To assess the efficacy of retinal tracer uptake and transport, we also examined the WGA-HRP labeling patterns in coronal section through the thalamus and superior colliculus (SC). Consistent with previous studies showing that ipsilateral retinal projections are weaker in albino than in pigmented rats (Lund, 1965; Lund, Lund, & Wise, 1974), the ipsilateral retinal projection fields are smaller in the dorsal lateral geniculate nucleus (LGN) of albino rats compared with those in Long Evans rats (cf. right LGNs in Figure 1g,h). Contralaterally, the labeling was uniformly dense throughout the LGN, except for small dorsomedial regions where the labeling was reduced, presumably corresponding to the ipsilateral eye recipient zone. In the SC, the contralateral projections in both rat strains was dense and uniform throughout the nucleus, while the ipsilateral projection was weaker in the albino strain (cf. Figure 1g,h). These labeling patterns provide evidence that the tracer was taken up and transported evenly by the entire retina following intraocular injections of WGA-HRP. Figure 1i shows higher magnification views of the ipsilateral LGN labeling pattern from the Long Evans and albino rats, displayed in (g), (h), respectively. Arrows illustrate that a region located dorsomedially to the target of ipsilateral eye projections remains unlabeled after an

injection of WGA-HRP into the ipsilateral eye. This region provides direct input to lateral striate cortex in both rat strains (Lewis & Olavarria, 1995; Olavarria & Hiroi, 2003), and the fact that it remains unlabeled after an ipsilateral eye injection is consistent with our observation that the LS in albino rats does not receive significant direct input from the ipsilateral eye (Figure 1c).

In Long Evans rats, the ipsilateral eye projections segregate into densely labeled patches of different sizes and shapes, arranged anteroposteriorly into either single or double strings (Figure 2a,b). In contrast, we found that the labeling of ipsilateral eye projections in albino rats was typically less dense and distributed more diffusely and homogeneously across the CS. These differences are appreciated more vividly in the 3D surface plots (Figure 2a-d, bottom panels) of the labeling density distributions within the rectangular areas demarcated by white segmented lines in each corresponding case in Figure 2a-d (top panels). In these plots, the z-axis represents the pixel value at each location.

To quantify the differences in the ipsilateral labeling segregation in the CS of Long Evans and albino rats, we took advantage of the fact that the surface area of the 3D labeling landscapes increases as the

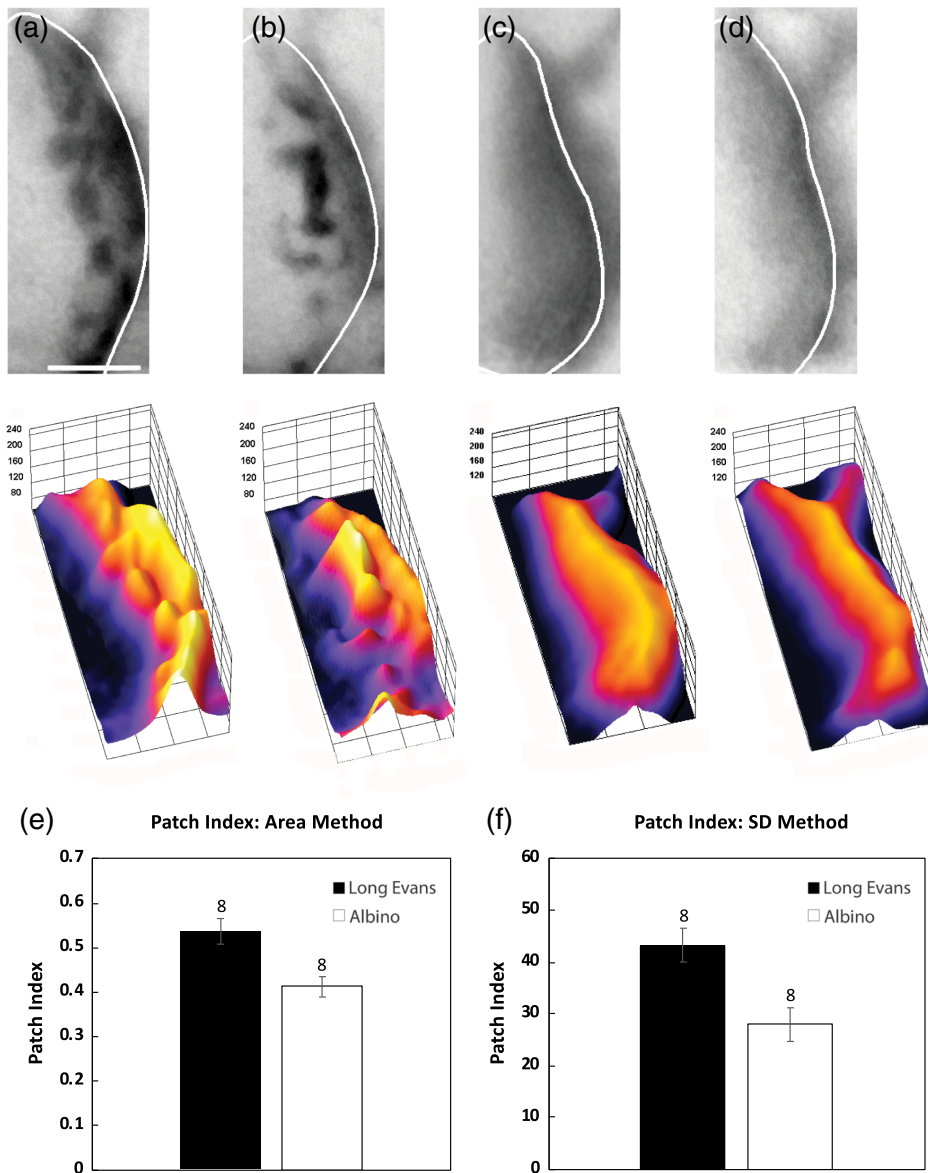
patchiness of the labeling distribution increases. We defined a PIA such that $PIA = 1 - SM/SI$, where SI is the surface area of the 3D density landscape in the analyzed CS region, while SM is the surface area of the projection of SI onto a 2D plane. Values of PIA approaching zero indicate low patchiness, while higher values of PIA indicate larger or more numerous fluctuations in the labeling density landscape (see Materials and Methods). The average PIA for Long Evans rats was 0.162 ($SEM = 0.01$, $n = 9$), while the PIA for albino rats was 0.102 ($SEM = 0.011$, $n = 7$) (Figure 2e), and this difference between both groups was statistically significant ($t_{14} = 3.839$, $p = .002$).

The degree of patchiness in ipsilateral WGA-HRP labeling was also compared between Long Evans and albino rats by calculating the SDs of the gray value distributions within a rectangular region in the CS (see Materials and Methods) and expressing these values as a SD patchiness index (PISD). We found a significant difference between the average PISD for Long Evans rats (6.934, $SEM = 0.585$) and albino rats (3.543, $SEM = 0.446$), ($t_{14} = 4.035$, $p = .001$) (Figure 2f). Together,

the results of both analyses suggest that the distribution of ipsilateral WGA-HRP labeling tends to be more diffuse in the CS of albino rats, and, if present, fluctuations in labeling density tend to be of low amplitude compared to those in the CS of Long Evans rats.

3.3 | Callosal connections

Patchiness of callosal connections in V1 was analyzed in eight Long Evans and eight albino rats using the patch indices used above for ipsilateral eye projections. Figure 3 shows the pattern of HRP-labeled callosal connections in two Long Evans rats (Figure 3a,b) and in two representative albino rats (Figure 3c,d). In the lower panels, Figure 3 shows the respective 3-D surface plots of callosal labeling in the CS and LS. In agreement with previous studies in rats (Cusick & Lund, 1981; Olavarria & van Sluyters, 1985), we observed that the distribution of callosal connections peaks at the border region between areas 17 and 18a, forming a band ~ 0.22 mm wide abutting the border of



V1 in both strains. The labeling in this band is homogeneous throughout its anteroposterior extent, with occasional less dense regions at one or two discrete sites in some cases. By its location and width, this lateral callosal band corresponds closely with the LS described above in albino rats and in Long Evans rats (Laing et al., 2015). From this band, callosal connections decrease in labeling density as they extend medially in both strains of rats, but while in Long Evans rats callosal connections form patches in the CS (Figure 3a,b) (Laing et al., 2015), the distribution is typically homogenous throughout the CS in albino rats (Figure 3c,d). Figure 3e shows that the average PIA was 0.536 ($SEM = 0.023$) for Long Evans rats, and 0.412 ($SEM = 0.028$) for albino rats, and this difference was statistically significant ($t_{14} = 3.389$, $p = .004$). There was also a significant difference in the SDs of the gray value distributions within the CS between Long Evans rats (43.259, $SEM = 3.428$) and albino rats (27.942, $SEM = 3.26$), ($t_{14} = 3.331$, $p = .005$) (Figure 3f).

3.4 | Electrophysiology

3.4.1 | The lateral segment is binocular in albino rats and monocular in Long Evans rats

Diao et al. (1983) reported that a region corresponding approximately to LS in lateral striate cortex of albino rats is highly binocular, while Laing et al. (2015) reported that evoked responses in the LS of Long Evans rats were strongly dominated by the contralateral eye. To directly examine whether these reported differences were due to the use of different rat strains, we compared the binocularity across CS and LS in 10 intact Long Evans rats and 5 albino rats.

Our results from Long Evans rats are in agreement with the electrophysiological and in situ hybridization findings of Laing et al. (2015), while our results in albino rats are in close agreement with those reported by Diao et al. (1983) in this rat strain. Our physiological results are consistent with our hypothesis that the physiological differences between Long Evans and albino rats reflect strain differences in the organization of retinal input and callosal connections in V1.

3.4.2 | Input from the ipsilateral eye to the lateral segment comes via the callosum in albino rats

Diao et al. (1983) proposed that ipsilateral input to lateral striate cortex comes via the callosum. To examine the contribution of the visual callosal pathway to the binocularity in V1 of albino rats, we recorded visually evoked responses in the CS and LS in 5 intact and 7 callosotomized albino rats. Recording sites across the different segments of V1 in an albino rat are illustrated with data from one tangential section in Figure 4a, and from a reconstruction using additional sections from the same case (Figure 4b). Figure 4c illustrates the effectiveness of the callosotomy.

To assess the ocular preference of evoked response at each recording site, a CBI was calculated from the counts of action potentials recorded for each trial. This index, defined as $CBI = (R_{contra} - R_{ipsi}) / (R_{contra} + R_{ipsi})$, ranges from -1 (purely ipsilateral response)

to $+1$ (purely contralateral response). Values ~ 0 indicate balanced binocular responses (see Materials and Methods).

We found that, in the LS (Figure 4e), evoked responses were highly binocular in intact albino rats ($CBI = 0.16$, $SEM = 0.049$), whereas responses were strongly dominated by the contralateral eye in Long Evans rats ($CBI = 0.74$, $SEM = 0.058$) ($t_{13} = 7.496$, $p < .001$). However, after callosotomy in albino rats, the contralateral eye became strongly dominant ($CBI = 0.82$, $SEM = 0.057$) ($t_{19} = 8.439$, $p < .001$), reaching a score similar to that of Long Evans rats ($t_{14} = 0.866$, $p = .401$). The fact that the influence of the contralateral eye in the LS is as high in Long Evans rats as in callosotomized albino rats provides compelling evidence that the bulk, if not all, of the input from the ipsilateral eye to the LS comes via the callosum in albino rats.

In the CS (Figure 4d), callosotomy in albino rats shifts the ocular dominance preference from being highly binocular ($CBI = 0.11$, $SEM = 0.07$) to being dominated by the contralateral eye ($CBI = 0.52$, $SEM = 0.09$), a difference that was significant ($t_{45} = 3.371$, $p = .002$). However, this shift is smaller than that observed in the LS after callosotomy (cf Figure 4e). This increase in contralateral eye dominance in the CS of albino rats after callosotomy likely reflects the strengthening of the contralateral retinal projection and weakening of the ipsilateral projection that characterizes albino rats (Lund, 1965; Lund et al., 1974). Due to this difference, the ipsilateral eye input to the CS relayed through the corpus callosum is stronger than that relayed through the direct ipsilateral input to the same CS (consider the direct and indirect ipsilateral eye input to the right CS in Figure 5b). The direct ipsilateral input would therefore be unable to compensate for the reduction in ipsilateral input caused by the transection of the corpus callosum, leading to a relative increase in contralateral eye dominance in the CS. In contrast, in Long Evans rats, the strength of the direct ipsilateral eye input to the CS appears to match that of the ipsilateral input relayed through the corpus callosum because transection of the corpus callosum does not change the binocularity in the CS (Laing et al., 2015). The relative strengthening of the ipsilateral eye input relayed through the callosum in albino rats may also explain our observation that the CS in intact albinos appears to be more binocular ($CBI = 0.11$) than the CS in intact Long Evans rats ($CBI = 0.33$, $SEM = 0.066$) ($t_{50} = 2.446$, $p = .018$) (Figure 4d). Finally, in Long Evans rats, the contralateral eye exerts some dominance in the CS ($CBI = 0.33$, $SEM = 0.066$) (Figure 4d), but not as strongly as in the LS ($CBI = 0.74$, $SEM = 0.058$) (Figure 4e), which is consistent with the report by Laing et al. (2015) that the LS in Long Evans rats is strongly, if not exclusively, dominated by the contralateral eye.

3.4.3 | Contralateral eye input may be less dominant in the binocular V1 region of long Evans rats than previously thought

Traditionally, the region encompassing areas corresponding to both the CS and LS in rats has been designated as the "binocular region" in rats and other species. While this is the case in albino rats (Diao et al., 1983; the present study), in Long Evans rats the binocular region is

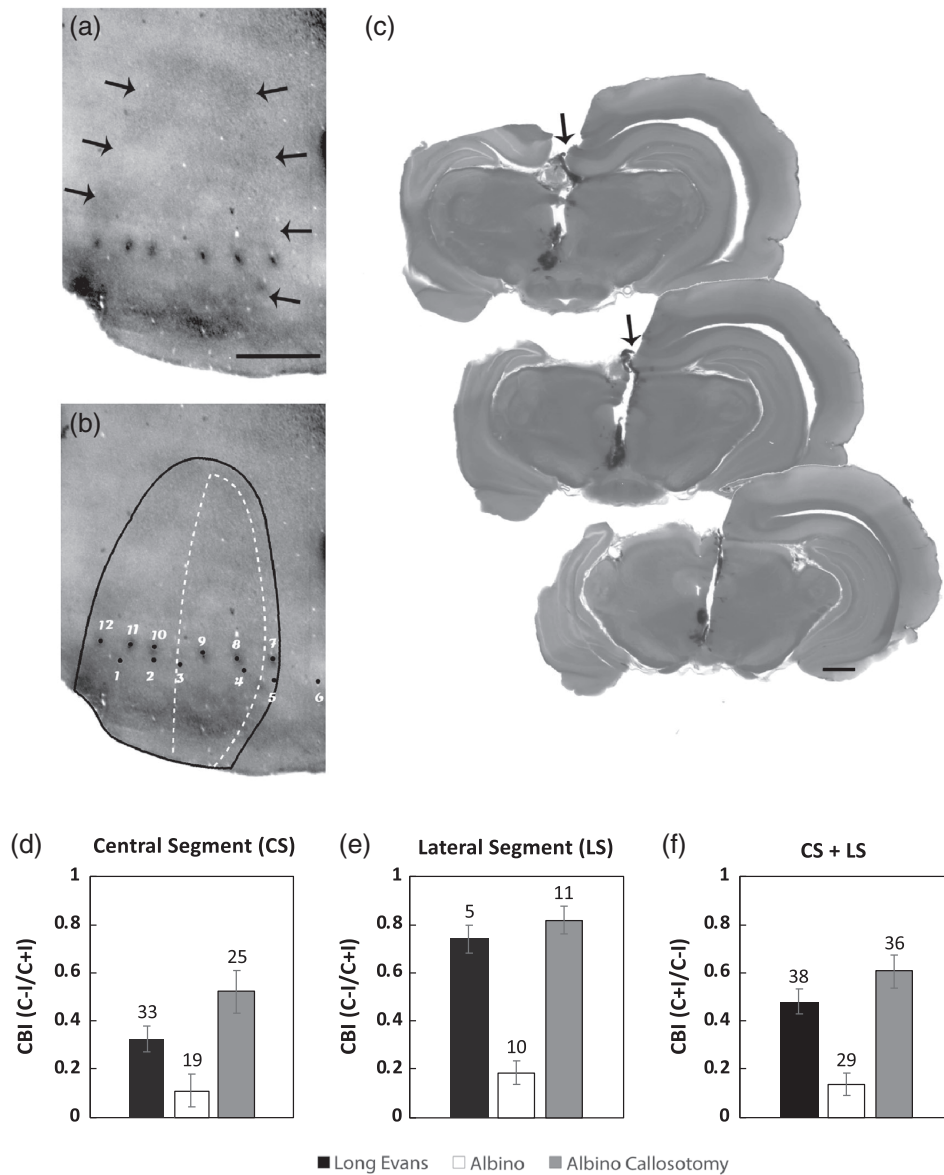


FIGURE 4 Recording sites in area V1 of albino rat. Callosotomy in albino rats. (a) Tangential section from callosotomized albino rat showing myelin pattern for V1 (arrows indicate the border of V1). Electrode penetrations (black dots) can be seen across V1. (b) Same section as in (a) showing border of V1 (black outline) and several additional electrode penetrations from same case in (a) identified after reconstruction from neighboring sections. The CS is outlined by white dashed line. This border was estimated using the information from cases analyzed as illustrated in Figure 1 (see Materials and Methods). (c) Coronal sections show transection of splenium of corpus callosum (arrows) in the top (anterior) two sections. The posterior section, at the level of the superior colliculus, demonstrates that the transection of splenium was complete. The left cortical mantle was removed for flattening and tangential sectioning. Scale bars = 1.0 mm. (d), (e), (f) quantitative analysis of binocularity in central and lateral segments of V1 in Long Evans and albino rats. (d) Central segment. In albino rats, callosotomy shifts the ocular dominance preference from highly binocular (CBI = 0.11, $n = 19$ recording sites) to dominated by the contralateral eye (CBI = 0.52, $n = 25$ recording sites). In Long Evans rats, the contralateral eye exerts some dominance (CBI = 0.33, $n = 33$ recording sites), but not as strongly as in the LS (b). (e) Lateral segment. Evoked responses were highly binocular in intact albino rats (CBI = 0.16, $n = 10$ recording sites). After callosotomy, dominance by the contralateral eye increased significantly (CBI = 0.82, $n = 11$ recording sites), reaching a score similar to that of Long Evans rats in the LS (CBI = 0.74, $n = 5$ recording sites). This shift is greater than that observed in the CS region of albino rats (d). (f) Pooling of data from the central and lateral segments. Long Evans ($n = 38$ recording sites), intact albino rats ($n = 29$ recording sites), and callosotomized albino rats ($n = 36$ recording sites)

restricted to the CS because the LS is nearly exclusively dominated by the contralateral eye (Laing et al., 2015, present study). Thus, previous estimations of the binocularity of V1 in Long Evans rats may have overestimated the influence of the contralateral eye because the

recordings probably have included sites within the LS. Indeed, in Long Evans rats we observed that the CBI obtained from recordings restricted to the CS (CBI = 0.33, SEM = 0.066, Figure 4d) was significantly smaller ($t_{58} = 2.135$, $p = .037$) than that obtained by pooling our

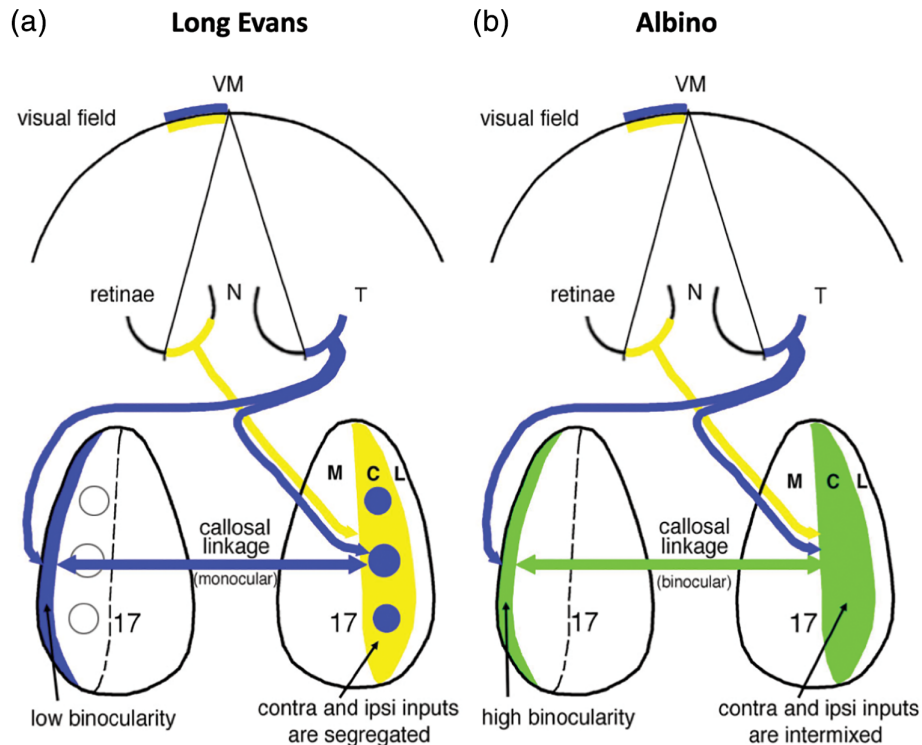


FIGURE 5 Influence of ODCs and patchy callosal connections on binocularity in the lateral segment of V1 (area 17). In both Long Evans and albino rats, callosal connections connect asymmetric, but topographically corresponding, loci in V1, such that opposite central and lateral segments connect reciprocally with each other (Lewis & Olavarria, 1995). (a) In Long Evans rats, ODCs and patchy callosal connections prevent the passage of ipsilateral eye input to the lateral segment. The left lateral segment (blue) cannot receive transcallosal input from the left, ipsilateral nasal retina (yellow) because the contralaterally dominated territory in the right central segment (yellow) is deprived of callosal connections (callosal patches correlate with ipsilateral ODCs, colored blue, Laing et al., 2015). (b) In contrast, we found that albino rats lack ODCs and patchy callosal connections. Thalamic inputs from right and left eyes are intermixed in the central segment (blue + yellow = green), allowing the callosal pathway to convey input from the ipsilateral eye to the lateral segment in the left hemisphere, thereby increasing binocularity in this segment (green). The same explanation applies to the right LS, not drawn for simplicity. C, central segment; L, lateral segment; M, medial segment

data from both the CS and LS ($CBI = 0.47$, $SEM = 0.053$, Figure 4f). In contrast, in intact albino rats, binocularity is relatively constant across both the CS and LS (Figure 4d,e), and pooling the data from these segments was not significantly different from recordings restricted to the CS (Figure 4f).

In summary, our data from LS in Long Evans rats support the finding by Laing et al. (2015) that LS is strongly dominated by input from the contralateral eye. Moreover, in agreement with Diao et al. (1983), our data from albino rats showed that evoked responses are predominantly binocular in LS of albino rats, and that transection of the callosum virtually eliminates input from the ipsilateral eye to this region.

4 | DISCUSSION

4.1 | The LS in albino rats is homologous to the LS in Long Evans rats

Albino rats are characterized by an increased crossed retinal projection and a reduced ipsilateral retinal projection (Lund, 1965; Lund et al., 1974). We were nevertheless able to identify the tripartite

subdivision of V1 described in Long Evans based on the distribution of WGA-HRP labeling following an intraocular injection of this tracer (Laing et al., 2015). In particular, between the CS, which receives the bulk of the input from the ipsilateral eye, and the lateral border of V1, we identified the LS as a narrow cortical strip where the tracer density was reduced or at background levels. Two additional observations provide further evidence that the LS in albino rats does not receive significant direct input from the ipsilateral eye: (a) in agreement with Diao et al. (1983), we observed that callosotomy abolished ipsilateral eye responses to lateral striate cortex; (b) lateral striate cortex in albino rats (Diao, Xiao, & Bu, 1987), as the LS in Long Evans rats (Adams & Forrester, 1968; Olavarria and Turecek, unpublished observations), represents ipsilateral visual fields. In both rat strains, this ipsilateral visual field representation is mediated by the contralateral projection from the temporal retina, which innervates a small dLGN region located dorsomedially to the target of the ipsilateral retinal projection (arrows in Figure 1i) (Reese & Cowey, 1987). This region provides input to lateral striate cortex in both rat strains (Lewis & Olavarria, 1995; Olavarria & Hiroi, 2003), and, as shown in Figure 1i (arrows), it remains unlabeled after a WGA-HRP injection into the

ipsilateral eye in both rat strains. Together, these observations provide strong support for the idea that LS in albino rats is homologous to LS in Long Evans rats.

4.2 | The presence of ODCs is associated with a reduction of binocularity in lateral V1

Diao et al. (1983) reported that in albino rats, ipsilateral eye responses can be recorded throughout the binocular zone and are especially robust in lateral striate cortex, in a region corresponding approximately to the LS. Our physiological recordings after transection of the corpus callosum confirmed the report by Diao et al. (1983) that ipsilateral input to this region is mediated by the callosal pathway. In contrast, in Long Evans rats, this region is nearly exclusively dominated by the contralateral eye despite being callosally connected (Laing et al., 2015). To explain why callosal connections are unable to convey ipsilateral eye input to the LS in Long Evans rats, we hypothesized that the development of ODCs renders callosal connections unable to relay indirect ipsilateral eye input to the LS. As illustrated in Figure 5a, the LS in the left hemisphere (blue strip) cannot receive transcallosal input from the retinotopically matched nasal retina in the ipsilateral eye (colored yellow) because nasal retina projects to regions in the contralateral V1 that are largely acallosal (colored yellow) due to the close association of callosal connections with *ipsilateral* ODCs (colored blue) (Laing et al., 2015). We therefore predicted that, instead of segregating into ODCs, ipsilateral and contralateral eye input intermix throughout the CS of albino rats, allowing the indirect, transcallosal transfer of ipsilateral eye input to lateral striate cortex. Figure 5b represents this prediction and illustrates that if both the yellow and blue eye-specific territories intermix in the right CS (blue + yellow = green), rather than segregate into ODCs, then input from the left hemiretina (yellow) arriving to the right CS (green) would have access to the left LS through the callosum, leading to an increased binocularity in the left LS. Based on the hypothesis that the distributions of eye-specific inputs and callosal connections are spatially coupled (Olavarria, 2001, 2002), we also predicted that callosal connections in albino rats would not be patchy as in Long Evans rats but would instead spread over the entire CS (green), reflecting the widespread distribution of ipsilateral eye thalamic input to the CS. Bearing out our predictions, our results from albino rats show that inputs from both eyes are largely intermixed throughout the CS, and callosal connections spread over the CS without forming distinct patches. It should be noted that a widespread distribution of callosal connections may not be necessary for the transcallosal transfer of ipsilateral eye input to the LS in albino rats. Callosal patches could still mediate such transfer because they would innervate areas of intermixed ipsilateral and contralateral eye input to the CS, allowing the ipsilateral eye to gain access to the LS via the callosum. Mice lack ODCs (Antonini, Fagiolini, & Stryker, 1999) and patchy callosal connections (Olavarria & van Sluyters, 1984), and a recent study reported that ipsilateral eye input to lateral striate cortex comes through the callosum in pigmented (C57BL/6) mice (Dehmel & Löwel, 2014). This report is consistent with our present results in albino rats and supports the corollary of our hypothesis, namely, that the absence

of ODCs and patchy callosal connections in V1 facilitate the passage of ipsilateral eye input to lateral striate cortex.

4.3 | Lack of ODCs in albino rats increases the size of the binocular region in V1

Our results extend the results of Diao et al. (1983) by showing that V1 in albino rats is subdivided into three segments, as in Long Evans rats (Laing et al., 2015). These segments consist of the medial, monocular segment (MS), dominated by the contralateral eye, the CS, receiving direct subcortical input from both eyes, and the LS, receiving primarily direct subcortical input from the contralateral eye (Figure 1). In each hemisphere, the MS and CS represent the contralateral visual hemifield, with the lateral border of the CS corresponding to the representation of the vertical meridian (VM) of the visual field. The LS extends this representation into the ipsilateral visual field (Adams & Forrester, 1968), which can reach up to 20–30 deg in albino rats (Diao et al., 1987). In this regard, the LS is analogous to the 17/18 transition zone in cats (Payne, 1990; Payne & Siwek, 1991), and lateral striate cortex in ferrets (White, Bosking, Williams, & Fitzpatrick, 1999). Moreover, consistent with the report of Diao et al. (1983), our results show that not only the CS, but also the LS, is binocular in albino rats, so that a more extensive region of cortex is binocular in albino rats compared to Long Evans rats. As illustrated in Figure 5, the binocular field is hemisected by the VM, and each half is represented only in the opposite CS in Long Evans rats, while in albino rats, each half of the binocular field is also represented in the ipsilateral LS. This increase in the area size of the binocular region implies that binocular neurons are probably more numerous in striate cortex of the albino strain, raising the possibility that albino rats may outperform Long Evans rats in some tasks requiring binocular vision. However, this possibility is not supported by behavioral studies of depth perception in albino and pigmented rats. For instance, Routtenberg and Glickman (1964) reported that albino rats perform worse than Long Evans rats in the cliff test, probably due to factors linked to albinism, such as lower visual acuity. Perhaps comparing the performance in the cliff test of *pigmented* mice, which lack both ODCs (Antonini et al., 1999) and patchy callosal connections (Olavarria & van Sluyters, 1984), with that of Long Evans rats may reveal an advantage of the “albino” organization in some binocular vision tests.

4.4 | Why do eye-specific inputs segregate into ODCs in long Evans rats but not in albino rats?

In albino rats, one would expect that ipsilateral eye projections to V1, although weaker than in Long Evans rats (Lund, 1965; Lund et al., 1974), would segregate, forming perhaps smaller or less densely labeled ocular dominance patches. Instead, we found that input from both eyes largely intermix throughout the CS, without segregating into distinct eye specific territories. It is possible that segregation of eye-specific domains requires the strength of ipsilateral eye input to rise above a certain threshold, below which segregation does not occur. However, reduction of ipsilateral eye input may not be a major

factor because pigmented animals with presumably normal ipsilateral projections can show characteristics similar to albino rats, namely, a binocular lateral striate cortex, and lack of both ODCs and patchy callosal connections (e.g., mice, Antonini et al., 1999; Olavarria & van Sluyters, 1984; tree shrews, Bosking, Kretz, Pucak, & Fitzpatrick, 2000). It is possible that mechanisms driving the development of either intermixed or segregated eye-specific domains are influenced by factors associated with albinism, and that these factors are also present in some pigmented species. This possibility is suggested by the recent finding that characteristics thought to be pathognomonic of albinism are also observed in the absence of any hypopigmentation (Ahmadi et al., 2018). Further comparative studies in albino rats and in other albino and pigmented strains may help in identifying factors associated with the characteristics of eye-specific input and callosal connections we observed in albino rats.

4.5 | Spatial coupling between the distributions of direct eye-specific inputs and callosal connections

Laing et al. (2015) showed in Long Evans rats that callosal connections form distinct patches that colocalize with ipsilateral ODCs in the CS. Our present results in albino rats show that neither ipsilateral eye input nor callosal connections segregate into distinct patches but nevertheless remain spatially correlated as they overlap throughout the CS. More generally, previous studies have shown that callosal connections in V1 are patchy in animals with ODCs (e.g., rat, Laing et al., 2015; cat, Olavarria, 2001), whereas in animals without ODCs, callosal connections are not patchy (e.g., pigmented mouse, Olavarria & van Sluyters, 1984; tree shrews, Casagrande & Harting, 1975; Cusick, MacAvoy, & Kaas, 1985). Thus, species without ODCs may resemble albino rats in that striate cortex is likely to be binocular in regions of lateral striate cortex corresponding to the LS in rats. Consistent with this, the binocular region appears to include lateral striate cortex in both pigmented mice (Antonini et al., 1999) and tree shrews (Bosking et al., 2000), species which lack ODCs. Conversely, studies in sheep (Pettigrew, Ramachandran, & Bravo, 1984) show that a region corresponding to the LS in lateral striate cortex is binocular, and that input from the ipsilateral eye to this region comes through the callosum. Thus, it is likely that sheep, like albino rats and pigmented mice, lack ODCs.

The observation that the distributions of ipsilateral eye input and callosal connections remain spatially coupled whether or not eye-specific inputs segregate into ODCs supports the idea that the distribution of callosal connections is specified by bilateral projections from temporal retina (Laing et al., 2015; Olavarria, 2001, 2002). This hypothesis explains why callosal connections correlate with ipsilateral eye domains in the CS of rats, and in the corresponding region of V1 in cats, but with contralateral eye domains in the LS of rats and its analogue in the cat: the 17/18 transition zone (Laing et al., 2015; Olavarria, 2001). As discussed above, the intermixing of ipsilateral and contralateral eye input throughout the CS would make it possible for ipsilateral eye input to reach the LS indirectly through the callosum even if callosal connections were patchy in the CS of albino rats. Nevertheless, the observation of widespread callosal connections in the CS of albino rats is

interesting because it is consistent with the spatial coupling predicted to exist between the distributions of eye-specific inputs and callosal connections in striate cortex in species either with (Laing et al., 2015; Olavarria, 2001) or without (present study) ODCs.

4.6 | Contribution of callosal connections toward the generation of binocular neurons

The contribution of callosal connections toward the generation of cortical binocular neurons is still a matter of debate. No clear picture has emerged from numerous studies that have used a variety of approaches to determine the extent to which binocularity in visual cortex depends on callosal input (reviewed in Olavarria, 2002). The hypothesis that callosal fibers preferentially link opposite cortical loci that are under the influence of bilateral projections from the same temporal retina (Olavarria, 2001, 2002) sheds light on this debate because it implies that callosal fibers are not primarily involved in generating binocular cells in striate cortex. As illustrated in Figure 5, callosal input to a cortical cell largely duplicates the subcortical input from one of the eyes to the same cell. This would allow the direct subcortical input to sustain the responses of cortical cells when callosal input is eliminated. This hypothesis leads to the prediction that sectioning the callosal commissure should not have a significant effect on the binocularity indices recorded in striate cortex of Long Evans rats and cats, in agreement with previous and recent reports (Long Evans rats: Laing et al., 2015; cat: Conde-Ocazionez et al., 2018; Minciacchi & Antonini, 1984). Although both cats (Anderson, Olavarria, & Van Sluyters, 1988) and Long Evans rats (Laing et al., 2015) have ODCs in V1, it is interesting to note that the LS of rats is essentially monocular, while the cat 17/18 transition zone is binocular. In cats, the ipsilateral eye input to the 17/18 transition zone comes via direct subcortical projections, rather than indirectly via the callosum (recall that callosal connections correlate with *contralateral* ODCs in the cat transition zone [Olavarria, 2001; reviewed in Olavarria, 2002]). This, and the observation that section of the callosum in cats does not reduce binocularity in the transition zone (Minciacchi & Antonini, 1984; Conde-Ocazionez et al., 2018) support our hypothesis that the inability of callosal connections to relay indirect input from the ipsilateral eye to lateral striate cortex in Long Evans rats is due to the existence of ODCs in striate cortex.

On the other hand, in some species, binocularity in lateral striate cortex does depend on callosal input, as shown in albino rats (Diao et al., 1983; present study), pigmented mice (Dehmel & Löwel, 2014), and sheep (Pettigrew et al., 1984). It is also known that callosal connections contribute to binocularity in some extrastriate areas in Siamese cats, animals in which ipsilateral striate-extrastriate projections are largely monocular (Marzi, Antonini, Di Stefano, & Legg, 1980; Zeki & Fries, 1980). These considerations suggest that generation of binocular cells cannot be regarded as a basic, defining function of visual callosal connections in all species, or in all visual areas. At least in striate cortex, whether callosal input contributes or not to the generation of binocular cells appears to depend on restrictions imposed by the relationship of callosal connections with the organization of

eye-specific projections, which in some species segregate into ODCs, and in other species do not.

5 | CONCLUSIONS

Our results show that, in contrast to Long Evans rats, direct eye-specific projections do not segregate into ODCs in albino rats. Whether this is related either to reductions in the strength of ipsilateral eye specific input, to factors related to albinism, or to other factors present in albino and some pigmented species, remains to be studied. We also found that callosal connections in striate cortex of albino rats do not aggregate into distinct patches as in Long Evans rats. Instead, callosal connections are distributed throughout the CS, overlapping the distribution of ipsilateral eye input in this segment. These results provide further evidence that the organization of callosal connections in V1 is closely coupled to the organization of eye-specific inputs, and that changes in the relative distribution of these inputs, that is, whether they segregate into ODCs or intermix in the CS, can profoundly impact the distribution and function of callosal connections in V1 (Olavarria, 2001, 2002). Our findings provide insight about the role of callosal connections in generating binocular cells and suggest that albino rats may be a useful model for studying factors that regulate both the segregation of eye-specific input in mammalian visual cortex, as well as the spatial correlation between eye-specific domains and callosal connections in striate cortex.

ACKNOWLEDGMENTS

This work was supported in part by a Royalty Research Fund award, University of Washington to JFO, and by National Institutes of Health grant R01NS070022. AKA & RJL were supported by National Institute of Health Vision Training Grant T32 EY7031.

CONFLICT OF INTEREST

The authors declare no potential conflict of interest.

AUTHORS CONTRIBUTION

Authors had full access to the data and take responsibility for the integrity of the data and analysis. Concept and design: AKA, RJL, JFO. Data acquisition: AKA, ZD, RJL, JT. Analysis and interpretation of data: AKA, BL, JFO.

DATA AVAILABILITY STATEMENT

The data that support the findings of this study are available from the corresponding author upon reasonable request.

ORCID

Jaime F. Olavarria  <https://orcid.org/0000-0001-5211-7970>

REFERENCES

- Adams, A. D., & Forrester, J. M. (1968). The projection of the rat's visual field on the cerebral cortex. *Quarterly Journal of Experimental Physiology*, 53(3), 327–336.
- Ahmadi, K., Fracasso, A., van Dijk, J. A., Kruijt, C., van Genderen, M., Dumoulin, S. O., & Hoffmann, M. B. (2018). Altered organization of the visual cortex in FHONDA syndrome. *NeuroImage*, 190, 224–231. doi:<https://doi.org/10.1016/j.neuroimage.2018.02.053>.
- Anderson, P. A., Olavarria, J., & Van Sluyters, R. C. (1988). The overall pattern of ocular dominance bands in cat visual cortex. *The Journal of Neuroscience*, 8(6), 2183–2200.
- Antonini, A., Fagiolini, M., & Stryker, M. P. (1999). Anatomical correlates of functional plasticity in mouse visual cortex. *The Journal of Neuroscience*, 19(11), 4388–4406.
- Bosking, W. H., Kretz, R., Pucak, M. L., & Fitzpatrick, D. (2000). Functional specificity of callosal connections in tree shrew striate cortex. *The Journal of Neuroscience*, 20(6), 2346–2359.
- Casagrande, V. A., & Harting, J. K. (1975). Transneuronal transport of tritiated fucose and proline in the visual pathways of tree shrew *Tupaia glis*. *Brain Research*, 96(2), 367–372.
- Conde-Ocazonez, S. A., Jungen, C., Wunderle, T., Eriksson, D., Neuenschwander, S., & Schmidt, K. E. (2018). Callosal influence on visual receptive fields has an ocular, an orientation-and direction bias. *Frontiers in System Neuroscience*, 12(11), 1–13. <https://doi.org/10.3389/fnsys.2018.00011>
- Cusick, C. B., & Lund, R. D. (1981). The distribution of the callosal projection to the occipital visual cortex in rats and mice. *Brain Research*, 214(1), 239–259.
- Cusick, C. G., MacAvoy, M. G., & Kaas, J. H. (1985). Interhemispheric connections of cortical sensory areas in tree shrews. *The Journal of Comparative Neurology*, 235(1), 111–128.
- Dehmel, S. & Löwel, S. (2014). Cortico-cortical interactions influence binocularity of the primary visual cortex of adult mice. *PLoS One*, 9(8), e105745. doi: 10.1371/journal.pone.0105745.
- Diao, Y. C., Wang, Y. K., & Pu, M. L. (1983). Binocular responses of cortical cells and the callosal projection in the albino rat. *Experimental Brain Research*, 49(3), 410–418.
- Diao, Y. C., Xiao, Y. M., & Bu, M. L. (1987). Callosal projections in the visual cortex and the vertical meridian of the visual field in the albino rat. *Scientia Sinica, Series B*, 30(2), 141–148.
- Itaya, S. K., & van Hoesen, G. W. (1982). WGA-HRP as a transneuronal marker in the visual pathways of monkey and rat. *Brain Research*, 236(1), 199–204.
- Kageyama, G. H., Gallivan, M. E., Gallardo, K. A., & Robertson, R. T. (1990). Relationships between patterns of acetylcholinesterase activity and geniculocortical terminal fields in developing and mature rat visual cortex. *Developmental Brain Research*, 53(1), 139–144.
- Laing, R. J., Bock, A. S., Lasiene, J., & Olavarria, J. F. (2012). Role of retinal input on the development of striate-extrastriate patterns of connections in the rat. *The Journal of Comparative Neurology*, 520(1), 3256–3276.
- Laing, R. J., Turecek, J., Takahata, T., & Olavarria, J. F. (2015). Identification of eye-specific domains and their relation to callosal connections in primary visual cortex of Long Evans rats. *Cerebral Cortex*, 25(10), 3314–3329.
- Lewis, J. W., & Olavarria, J. F. (1995). Two rules for callosal connectivity in striate cortex of the rat. *The Journal of Comparative Neurology*, 361(1), 119–137.
- Lund, R. D. (1965). Uncrossed visual pathways of hooded and albino rats. *Science*, 149(3691), 1506–1507.
- Lund, R. D., Lund, J. S., & Wise, R. P. (1974). The organization of the retinal projection to the dorsal lateral geniculate nucleus in pigmented and albino rats. *The Journal of Comparative Neurology*, 158(4), 383–403.

- Marzi, C. A., Antonini, A., Di Stefano, M., & Legg, C. R. (1980). Callosum-dependent binocular interactions in the lateral suprasylvian area of Siamese cats which lack binocular neurons in areas 17 and 18. *Brain Research*, 197(1), 230–235.
- Mesulam, M. M. (1978). Tetramethyl benzidine for horseradish peroxidase neurohistochemistry: A non-carcinogenic blue reaction product with superior sensitivity for visualizing neural afferents and efferents. *Journal of Histochemistry and Cytochemistry*, 26(2), 106–117.
- Minciacchi, D., & Antonini, A. (1984). Binocularity in the visual cortex of the adult cat does not depend on the integrity of the corpus callosum. *Behavioral Brain Research*, 13(2), 183–192.
- Olavarria, J. F., & Hiroi, R. (2003). Retinal influences specify cortico-cortical maps by postnatal day six in rats and mice. *The Journal of Comparative Neurology*, 459(2), 156–172.
- Olavarria, J. F. (2001). Callosal connections correlate preferentially with ipsilateral cortical domains in cat areas 17 and 18, and with contralateral domains in the 17/18 transition zone. *The Journal of Comparative Neurology*, 433(4), 441–457.
- Olavarria, J. F. (2002). Influence of topography and ocular dominance on the functional organization of callosal connections in cat striate cortex. In B. Payne & A. Peters (Eds.), *The cat primary visual cortex* (pp. 259–294). New York, NY: Academic Press.
- Olavarria, J. F., & van Sluyters, R. C. (1984). Callosal connections of the posterior neocortex in normal-eyed, congenitally anophthalmic, and neonatally enucleated mice. *The Journal of Comparative Neurology*, 230(2), 249–268.
- Olavarria, J. F., & van Sluyters, R. C. (1985). Organization and postnatal development of callosal connections in the visual cortex of the rat. *The Journal of Comparative Neurology*, 239(1), 1–26.
- Payne, B. R. (1990). Function of the corpus callosum in the representation of the visual field in cat visual cortex. *Visual Neuroscience*, 5(2), 205–211.
- Payne, B. R., & Siwek, D. F. (1991). Visual-field map in the callosal recipient zone at the border between areas 17 and 18 in the cat. *Visual Neuroscience*, 7(3), 221–236.
- Pettigrew, J. D., Ramachandran, V. S., & Bravo, H. (1984). Some neural connections subserving binocular vision in ungulates. *Brain, Behavior and Evolution*, 24(2–3), 65–93.
- Reese, B. E., & Cowey, A. (1987). The crossed projection from the temporal retina to the dorsal lateral geniculate nucleus in the rat. *Neuroscience*, 20(3), 951–959.
- Richter, C. P., & Warner, C. L. (1974). Comparison of Weigert stained sections with unfixed, unstained sections for study of myelin sheaths. *Proceedings of the National Academy of Sciences of the United States of America*, 71(3), 598–601.
- Routtenberg, A., & Glickman, S. E. (1964). Visual cliff behavior in albino and hooded rats. *Journal of Comparative and Physiological Psychology*, 58(1), 140–142.
- Trojanowski, J. Q., Gonatas, J. O., & Gonatas, N. K. (1981). A light and electron microscopic study of the intraneuronal transport of horseradish peroxidase and wheat germ agglutinin-peroxidase conjugates in the rat visual system. *Journal of Neurocytology*, 10(3), 441–456.
- White, L. E., Bosking, W. H., Williams, S. M., & Fitzpatrick, D. (1999). Maps of central visual space in ferret V1 and V2 lack matching inputs from the two eyes. *The Journal of Neuroscience*, 19(16), 7089–7099.
- Zeki, S., & Fries, W. (1980). A function of the corpus callosum in the Siamese cat. *Proceeding of the Royal Society of London B: Biological Sciences*, 207(1167), 249–258.

How to cite this article: Andelin AK, Doyle Z, Laing RJ, Turecek J, Lin B, Olavarria JF. Influence of ocular dominance columns and patchy callosal connections on binocularity in lateral striate cortex: Long Evans versus albino rats. *J Comp Neurol*. 2020;528:650–663. <https://doi.org/10.1002/cne.24786>